Journal of Organometallic Chemistry 904 (2019) 121015

Contents lists available at ScienceDirect

Journal of Organometallic Chemistry

journal homepage: www.elsevier.com/locate/jorganchem

DFT study on the rhodium-catalyzed oxidative C–H allylation of benzamides with 1,3-dienes by ally-to-ally 1,4-Rh(III) migration

Shaojing Liu [a, b], Daojun Guo [a, **], Tao Liu [a, b, *]

[a] School of Chemistry and Chemical Engineering, Qufu Normal University, Qufu, 273165, Shandong Province, People's Republic of China
[b] Department of Chemistry and Chemical Engineering, Jining University, Qufu, 273155, Shandong Province, People's Republic of China

ARTICLE INFO

Article history:
Received 9 October 2019
Received in revised form
31 October 2019
Accepted 1 November 2019
Available online 4 November 2019

Keywords:
DFT
C–H activation
1,4-Rh migration

ABSTRACT

The reaction mechanisms of Rh-catalyzed C–H allylation of benzamide with 1,3-diene were investigated by employing the density functional theory (DFT) calculations. Five main steps are included in this reaction: N–H bond activation, C–H bond activation, olefin insertion, 1,4-Rh migration, and β-hydride elimination. The rate-determining step is β-hydride elimination according to our calculations. Lam et al. have proposed three possible mechanisms for the 1,4-Rh migration, but the barriers are calculated to be high. In contrast, the H-migration process from methyl group to N center and to C4 center successively is the most feasible one, consistent with the deuterium transfer experiment.

© 2019 Elsevier B.V. All rights reserved.

1. Introduction

Transition-metal-catalyzed C–H functionalization [1] can be used to synthesize complex molecules with simple starting material due to its green and economic characteristics, which has become a useful tool for synthetic chemistry [2]. In these reactions, the step of 1,4-metal migration, where a carbon-bonded metal is exchanged with the hydrogen on the fourth carbon, has attracted more and more attention during the past few decades [3]. This isomerization can form subsequent C–C bond at sites different from the traditional location. Although the allyl-to-allyl 1,4-Rh(I) migration of allylrhodium(I) species have been extensively described [4–6], the allyl-to-allyl 1,4-Rh(III) migration is rarely studied.

Recently, Lam et al. [7] reported the rhodium-catalyzed oxidative C–H allylation of benzamides with 1,3-dienes (Scheme 1). The possible reaction mechanisms postulated by Lam and co-workers are summarized in Scheme 2. As shown in Scheme 2, the reaction begins with the generation of rhodacycle **I** through the reacting of $Cp^*Rh(OAc)_2$ (**cat**), generated from $[Cp^*RhCl_2]_2$ and $Cu(OAc)_2$, with N-acetylbenzamide **R1**. Next, the coordination and insertion of 1,3-diene **R2'** at the less substituted olefin of **I** gives rhodacycle **II**. Acetolysis of **II** affords the allylrhodium (III) **III**. Allyl-to-allyl 1,4-Rh(III) migration of **III** then occurs to yield a new allylrhodium species **IV**. Lam et al. proposed three possible 1,4-Rh migration pathways from **III** to **IV** based on the deuterated experiment. In path A, concerted metalation-deprotonation of **III** promoted by acetate takes place firstly to produce **III-IV^a**, followed by the acetolysis of **III-IV^a** to generate **IV**. Path B undergoes the successive C–H oxidative addition and reductive elimination process to form **IV**. In path C, **III** would transform into **IV** via a σ-complex-assisted metathesis (σ-CAM) transition state **TS-III-IV^c**. In the next step, isomerization of **IV** would bring intermediate **V**, which undergoes a β-hydride elimination to give product **P** and Cp*Rh(OAc)H. Through the subsequent oxidization of $Cu(OAc)_2$, catalyst is regenerated.

Although a plausible mechanistic pathway has been proposed by Lam group, the detailed reaction mechanism, especially the 1,4-Rh migration pathway, still need to be further discussed. Here we would like to report our detailed density functional theory (DFT) calculations on the reaction mechanisms. We expect this work would help understand the detailed mechanisms and design new related reactions.

2. Computational details

All structures were optimized and characterized as minima or transition states at the B3LYP [8]/BSI level (BSI designates the basis set combination of LanL2DZ [9] for Rh atom, and 6-31G (d,p) for

* Corresponding author. Department of Chemistry and Chemical Engineering, Jining University, Qufu, 273155, Shandong Province, People's Republic of China.
** Corresponding author.
E-mail addresses: guodaojun@qfnu.edu.cn (D. Guo), liutao_2005@126.com (T. Liu).

https://doi.org/10.1016/j.jorganchem.2019.121015
0022-328X/© 2019 Elsevier B.V. All rights reserved.

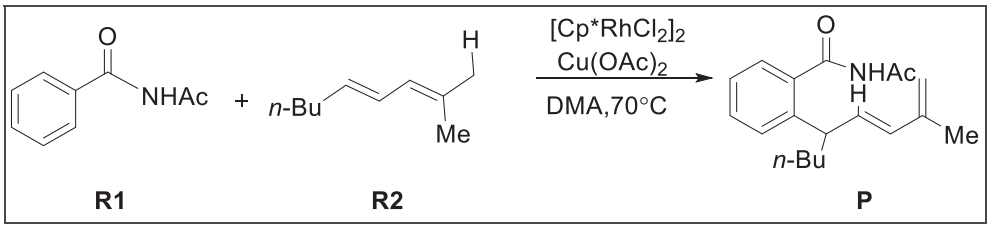

Scheme 1. The rhodium-catalyzed oxidative C–H allylation of benzamides with 1,3-dienes reported by Lam et al.

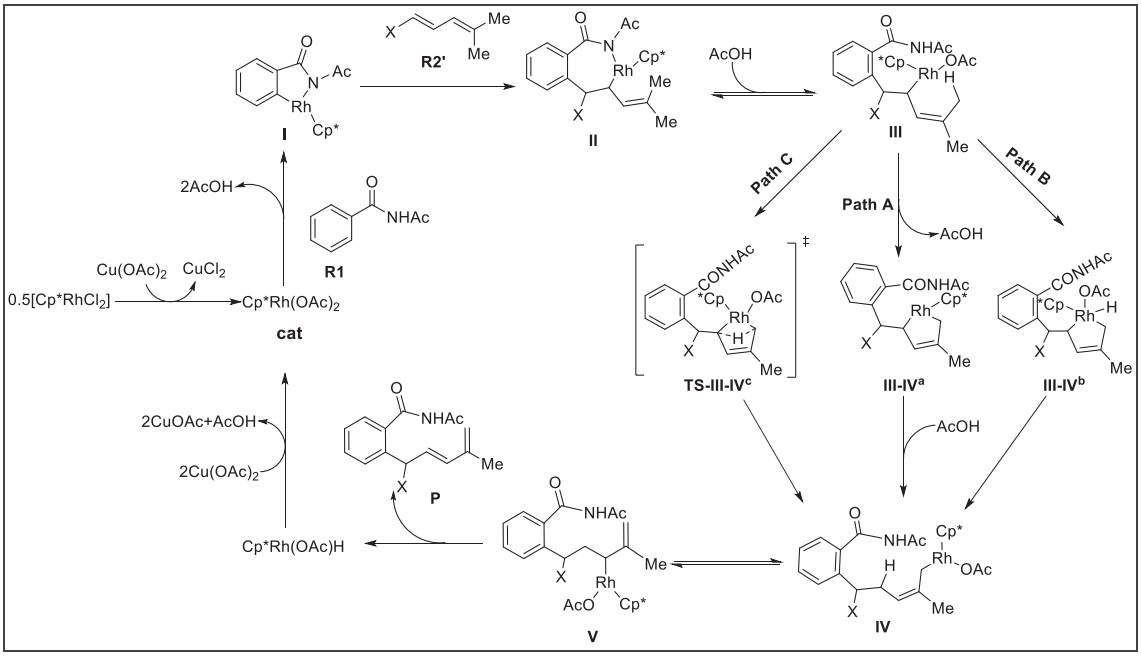

Scheme 2. The postulated mechanism reported by Lam and co-workers [7].

other atoms) in the gas phase. Frequency analysis was performed to ensure the stationary point as minimum or transition state at the B3LYP/BSI level. Intrinsic coordinate reaction (IRC) [10] calculations were carried out to examine the connectivity of a transition state with its backward and forward minima when necessary. The energetic results were then further refined by single-point calculations at the M06/BSII [11] level with solvation effects accounted for by the SMD [12] solvent model using N,*N*-dimethylacetamide (DMA) as solvent according to the experimental condition, where BSII denotes the basis set combination of SDD [13] for Rh atom and 6–311++G (d,p) for the remaining atoms. In all of the figures that contain free energy diagrams, calculated relative Gibbs

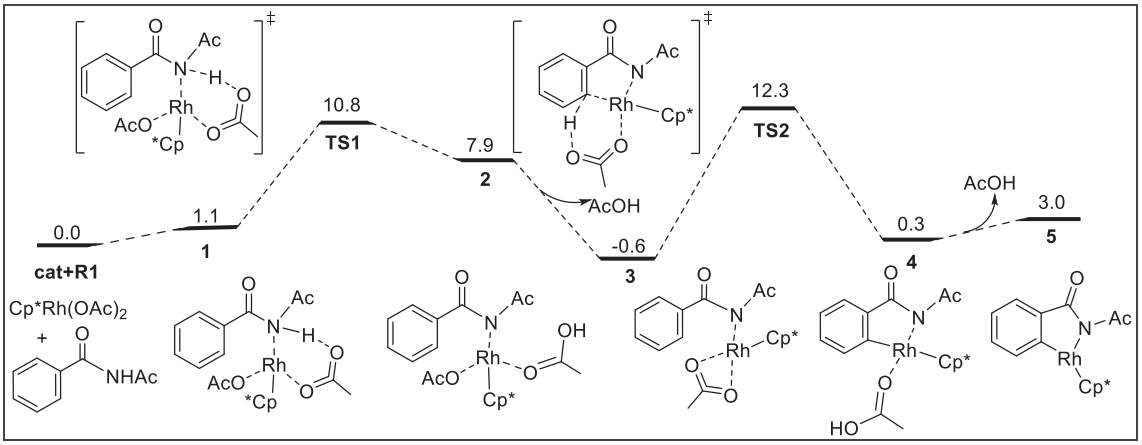

Fig. 1. Free energy profiles of N–H and C–H bond activation steps. The relative free energies are given in kcal/mol.

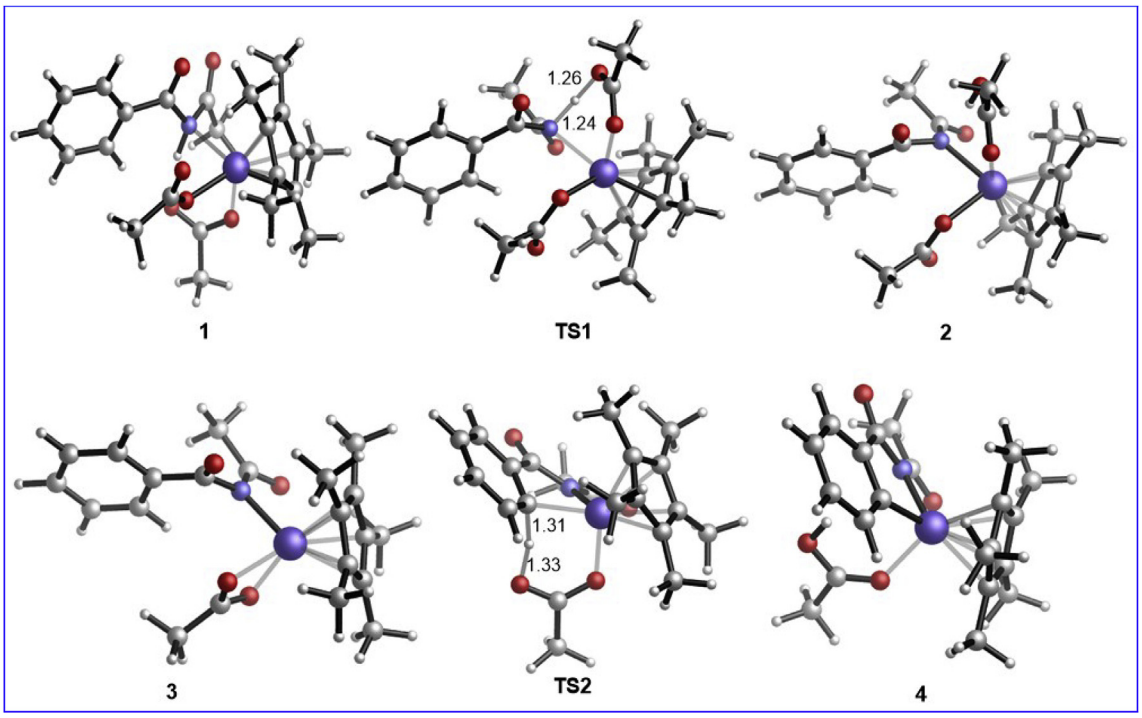

Fig. 2. The structures of key intermediates and transition states involved in the reaction mechanisms show in Fig. 1. The distances are given in Å.

free energies (kcal/mol) are presented. All the calculations were performed with the Gaussian 09 [14] software package.

3. Results and discussion

The mechanisms of the C–H allylation of **R1** with 1,3-diene **R2** catalyzed by **cat** are presented in Figs. 1, 3 and 5. The structures of key intermediates and transition states involved in the reaction mechanisms are listed in Figs. 2, 4 and 6. The N–H and C–H bond activation steps of **R1** are shown in Fig. 1. At the entrance of the reaction, catalyst **cat** coordinates to **R1** resulting into intermediate **1**, which is followed by the N–H bond cleavage to generate intermediate **2** via transition state **TS1** by consuming the activation barrier of 9.7 kcal/mol. A more stable intermediate **3** is then formed through the releasing of AcOH from **2**. Subsequently, a coordinated metallization deprotonation (CMD) C–H bond activation [15] takes place to afford intermediate **4** through transition state **TS2** with the barrier of 12.9 kcal/mol. The possible pathway of C–H activation prior to the N–H activation was also considered, but the calculated high barrier precludes this possibility (see Fig. S1 in the Supporting Information).

The **R2** insertion and 1,4-Rh migration processes are given in Fig. 3. The less substituted olefin of **R2** inserting into the Rh–C bond of **5** would lead to intermediate **6** via transition state **TS3** with the barrier of 13.9 kcal/mol. Other infeasible olefin insertion pathways are listed in Fig. S2 in Supporting Information.

For the subsequent 1,4-Rh migration, Lam et al. proposed three possible pathways based on the deuterated experiment as shown in Scheme 2, but all the free energies are calculated to be high (Fig. S3 in Supporting Information). Thus, a more favorable pathway is

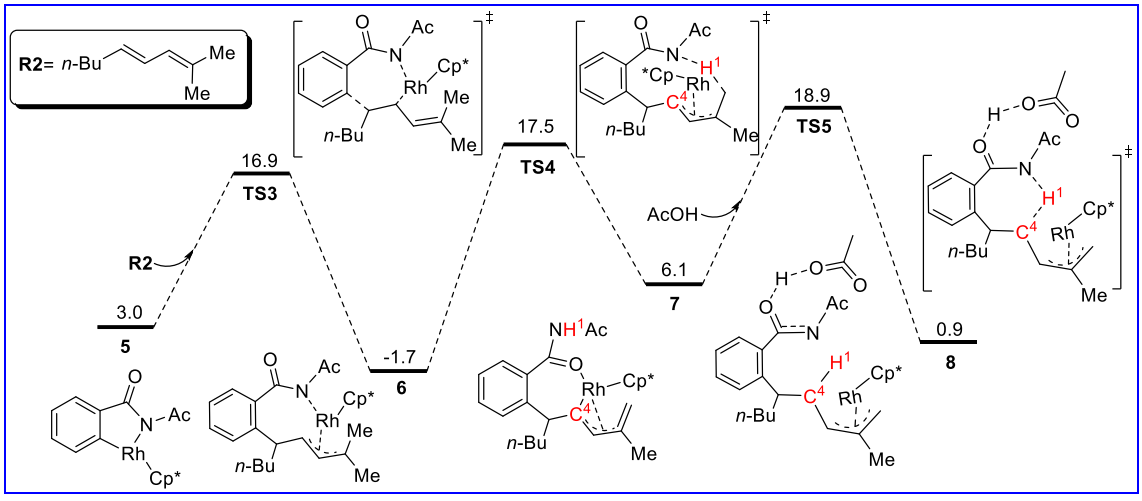

Fig. 3. Free energy profiles of olefin insertion and 1,4-Rh migration processes. The relative free energies are given in kcal/mol.

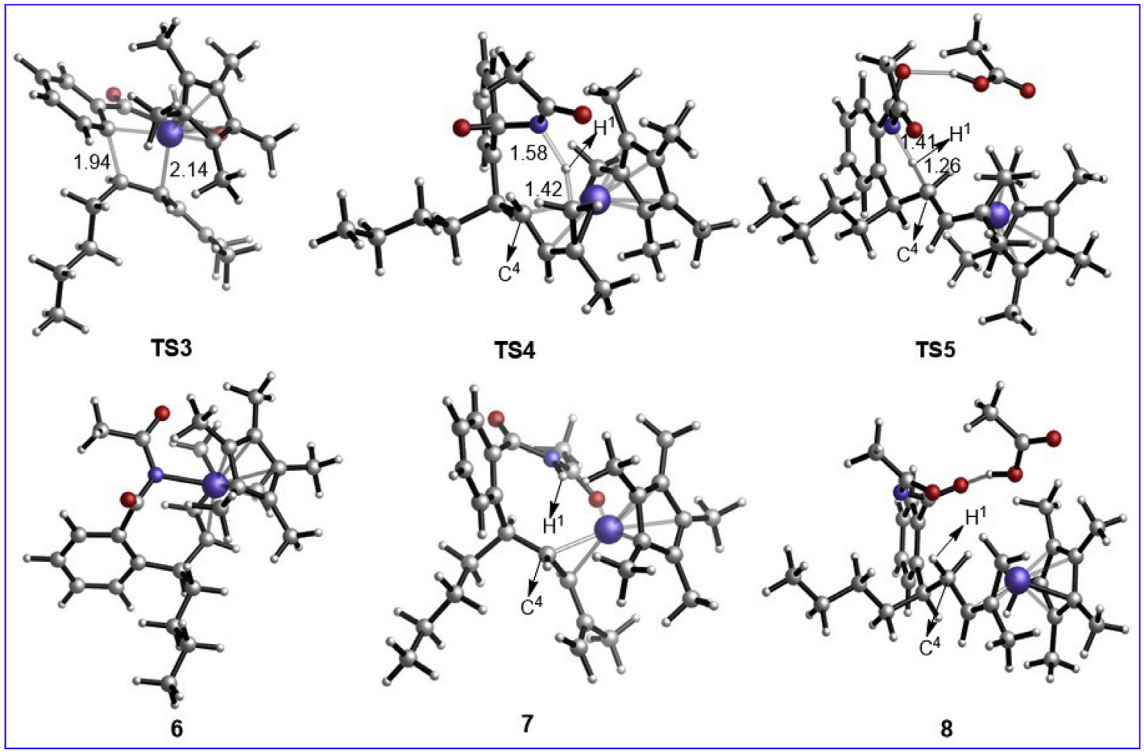

Fig. 4. The structures of key intermediates and transition states involved in the reaction mechanisms show in Fig. 3. The distances are given in Å.

expected. In fact, for the subsequent 1,4-Rh migration process, the H-migration (H^1 atom) firstly occurs from methyl group to the N center to afford intermediate **7** through transition state **TS4** (see Fig. 4). The free energy barrier for this step is 19.2 kcal/mol. The H1 atom in N center then migrates to C4 atom by crossing a barrier of 12.8 kcal/mol (**TS5** relative to **7**) to yield intermediate **8**. The calculated results are consistent with the deuterium transfer experiment. Other unfavorable H-migration processes are also

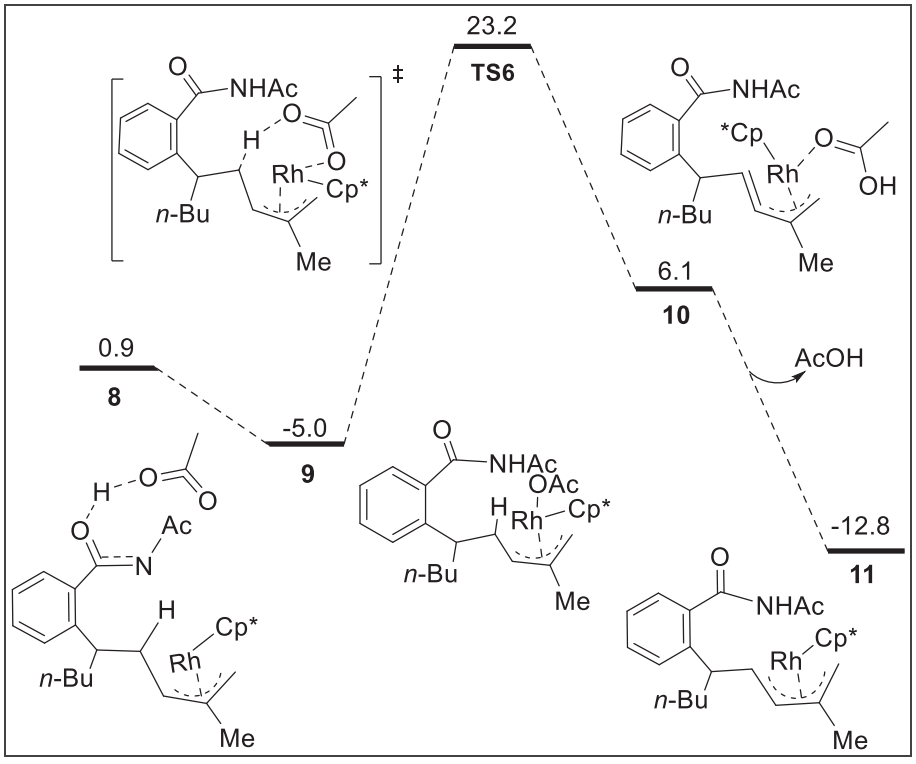

Fig. 5. Free energy profiles of β-hydride elimination step. The relative free energies are given in kcal/mol.

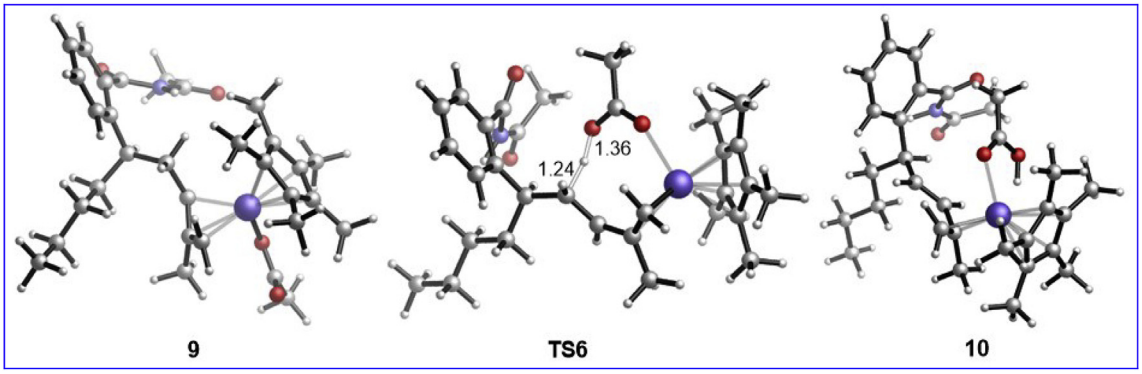

Fig. 6. The structures of key intermediates and transition states involved in the reaction mechanisms show in Fig. 5. The distances are given in Å.

calculated and ruled out due to the higher barriers (Figs. S4–S6 in Supporting Information).

The final β-hydride elimination step is shown in Fig. 5. N center of **8** is firstly protonated by the AcOH moiety attached to carbonyl group to afford a more stable intermediate **9**. Then the β-hydride elimination occurs to form intermediate **10** by overcoming the free energy barrier of 28.2 kcal/mol (**TS6**). Finally, the product complex **11** is produced through the releasing of acetic acid. As shown in Figs. 1, 3 and 5, the rate-determining step is the β-hydride elimination and the overall free energy barrier is 28.2 kcal/mol, in agreement with the experimental conditions.

4. Conclusions

By using DFT calculation, we have investigated the detailed mechanisms of Rh-catalyzed C–H allylation of benzamide with 1,3-diene. Based on our calculated results, the favorable reaction mechanism is given in Scheme 3, including five main steps: N–H

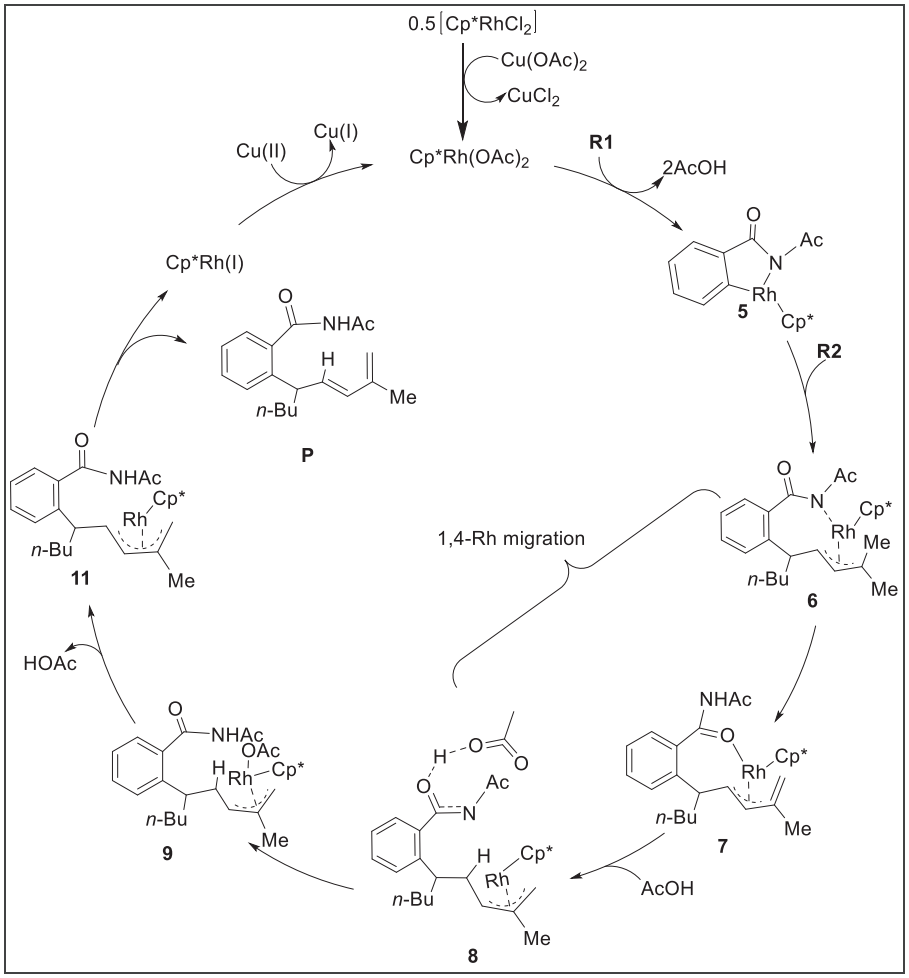

Scheme 3. The most favorable mechanism for this reaction according to our calculations.

activation, C–H activation, olefin insertion, 1,4-Rh migration, and β-hydride elimination. The β-hydride elimination is calculated to be the rate-determining step. For the 1,4-Rh migration step, the successive H-migration process from methyl group to N center and then to C4 center is calculated to be more favorable than the three possible mechanisms proposed by Lam et al.

Declaration of competing interest

The authors declare no conflict of interest.

Acknowledgements

This work was jointly supported by the National Natural Science Foundation of China (Nos. 21803024 and 21903038), and the Natural Science Foundation of Shandong Province (No. ZR2018LB016).

Appendix A. Supplementary data

Supplementary data to this article can be found online at https://doi.org/10.1016/j.jorganchem.2019.121015.

References

[1] (a) X.F. Fan, H.J. Zhao, J.J. Yu, X.G. Bao, C. Zhu, Org. Chem. Front. 3 (2016) 227–232;
(b) C. Zhang, C.M. Liu, Y. Shao, X.G. Bao, X.B. Wan, Chem. Eur J. 19 (2013) 17917–17925;
(c) C.L. Wang, Y.F. Zhou, X.G. Bao, J. Org. Chem. 82 (2017) 3751–3759.
[2] (a) M.L. Louillat, F.W. Paturneau, Chem. Soc. Rev. 43 (2014) 901–910;
(b) S.A. Girard, T. Knauber, C.J. Li, Angew. Chem. Int. Ed. 53 (2014) 74–100;
(c) T. Liu, S.W. Bi, Organometallics 35 (2016) 1114–1124;
(d) G. Rouquet, N. Chatani, Angew. Chem. Int. Ed. 52 (2013) 11726–11743;
(e) R. Kumar, E.V. Van der Eycken, Chem. Soc. Rev. 42 (2013) 1121–1146;
(g) G. Song, F. Wang, X. Li, Chem. Soc. Rev. 41 (2012) 3651–3678;
(f) K. Shin, S. Chang, J. Org. Chem. 79 (2014) 12197–12204;
(h) B.J. Li, Z.J. Shi, Chem. Soc. Rev. 41 (2012) 5588–5598;
(i) B. Li, P.H. Dixneuf, Chem. Soc. Rev. 42 (2013) 5744–5767.
[3] (a) S. Ma, Z. Gu, Angew. Chem. Int. Ed. 44 (2005) 7512–7517;
(b) Y. Ikeda, K. Takano, S. Kodama, Y. Ishii, Chem. Commun. 49 (2013) 11104–11106;
(c) F. Shi, R.C. Larock, Top. Curr. Chem. 292 (2010) 123–164.
[4] (a) K. Sasaki, T. Hayashi, Tetrahedron: Asymmetry 23 (2012) 373–380;
(b) T. Hayashi, K. Inoue, N. Taniguchi, M. Ogasawara, J. Am. Chem. Soc. 123 (2001) 9918–9919;
(c) R. Shintani, K. Okamoto, T. Hayashi, J. Am. Chem. Soc. 127 (2005) 2872–2873;
(d) T. Matsuda, M. Shigeno, M. Murakami, J. Am. Chem. Soc. 129 (2007) 12086–12087;
(e) M. Tobisu, I. Hyodo, M. Onoe, N. Chatani, Chem. Commun. 45 (2008) 6013–6015;
(f) T. Seiser, O.A. Roth, N. Cramer, Angew. Chem. Int. Ed. 48 (2009) 6302–6323;
(g) R. Shintani, S. Isobe, M. Takeda, T. Hayashi, Angew. Chem. Int. Ed. 49 (2010) 3795–3798.
[5] K. Oguma, M. Miura, T. Satoh, M. Nomura, J. Am. Chem. Soc. 122 (2000) 10464–10465.
[6] F. Shi, R.C. Larock, Top. Curr. Chem. 292 (2009) 123–164.
[7] S.E. Korkis, D.J. Burns, H.W. Lam, J. Am. Chem. Soc. 138 (2016) 12252–12257.
[8] (a) C. Lee, W. Yang, G. Parr, Phys. Rev. B 37 (1988) 785;
(b) P. Winget, T. Clark, J. Comput. Chem. 25 (2004) 725–733;
(c) P.J. Hay, W.R. Wadt, J. Chem. Phys. 82 (1985) 299;
(d) Y. Yang, Y. Liu, P. Lv, R. Zhu, C. Liu, D. Zhang, J. Org. Chem. 83 (2018) 2763–2772.
[9] (a) A.M. Mansour, O.R. Shehab, Inorg. Chem. Acta 480 (2018) 159–165;
(b) S. Esmaielzadeh, E. Zarenezhad, Acta Chim. Slov. 65 (2018) 416–428;
(c) Q. Wei, Y. Dai, C. Chen, L. Shi, Z. Si, Y. Wan, Q. Zuo, D. Han, Q. Duan, J. Mol. Struct. 1171 (2018) 786–792.
[10] (a) K. Fukui, Acc. Chem. Res. 14 (1981) 363–368;
(b) K. Yoshizawa, Y. Shiota, T. Yamabe, J. Chem. Phys. 111 (1999) 538–545;
(c) S. Maeda, Y. Harabuchi, M. Takagi, K. Suzuki, T. Lchino, Y. Sumiya, K. Sugiyama, Y. Ono, J. Comput. Chem. 39 (2018) 233–251.
[11] Y. Zhao, D.G. Truhlar, Theor. Chem. Acc. 120 (2008) 215–241.
[12] A.V. Marenich, C.J. Cramer, D.G. Truhlar, J. Phys. Chem. B 113 (2009) 6378–6396.
[13] (a) D. Andrae, U. Haeussermann, M. Dolg, H. Stoll, H. Preuss, Theor. Chim. Acta 77 (1990) 123–141;
(b) Y. Liu, C. Sun, S. Zhang, Theor. Chem. Acc. 132 (2013) 1–10;
(c) G.V. Barnett, V.I. Razinkov, B.A. Kerwin, T.M. Laue, A.H. Woodka, P.D. Butler, T. Perevozchikova, C.J. Roerts, J. Phys. Chem. B 119 (2015) 5793–5804.
[14] M.J. Frisch, G.W. Trucks, H.B. Schlegel, G.E. Scuseria, M.A. Robb, J.R. Cheeseman, G. Scalmani, V. Barone, B. Mennucci, G.A. Petersson, H. Nakatsuji, M. Caricato, X. Li, H.P. Hratchian, A.F. Izmaylov, J. Bloino, G. Zheng, J.L. Sonnenberg, M. Hada, M. Ehara, K. Toyota, R. Fukuda, J. Hasegawa, M. Ishida, T. Nakajima, Y. Honda, O. Kitao, H. Nakai, T. Vreven, J.A. Montgomery Jr., J.E. Peralta, F. Ogliaro, M. Bearpark, J.J. Heyd, E. Brothers, K.N. Kudin, V.N. Staroverov, R. Kobayashi, J. Normand, K. Raghavachari, A. Rendell, J.C. Burant, S.S. Iyengar, J. Tomasi, M. Cossi, N. Rega, N.J. Millam, M. Klene, J.E. Knox, J.B. Cross, V. Bakken, C. Adamo, J. Jaramillo, R. Gomperts, R.E. Stratmann, O. Yazyev, A.J. Austin, R. Cammi, C. Pomelli, J.W. Ochterski, R.L. Martin, K. Morokuma, V.G. Zakrzewski, G.A. Voth, P. Salvador, J.J. Dannenberg, S. Dapprich, A.D. Daniels, O. Farkas, J.B. Foresman, J.V. Ortiz, J. Cioslowski, D.J. Fox, Gaussian 09, Revision D.01, Gaussian Inc., Wallingford CT, 2009.
[15] (a) J. Zhang, C. H Shan, T. Zhang, J.S. Song, T. Liu, Y. Lan, Coord. Chem. Rev. 382 (2019) 69–84;
(b) J. Zhang, C.H. Shan, K. Lv, L. Zhu, Y.Y. Li, T. Liu, Y. Lan, ChemCatChem 11 (2019) 1228–1237;
(c) K. Lv, Y.Y. Jiang, L.L. Han, T. Liu, S.W. Bi, Mol. Catal. 462 (2019) 77–84;
(d) L.L. Han, X.Y. Ma, Y.X. Liu, Z.Y. Yu, T. Liu, Org. Chem. Front. 5 (2018) 725–733;
(e) L.L. Han, Y.P. Li, T. Liu, Dalton Trans. 47 (2018) 150–158.